






Article

Enhancing the Squareness and Bi-Phase Magnetic Switching of Co₂FeSi Microwires for Sensing Application

Mohamed Salaheldeen ^{1,2,3,4,*} , Asma Wederni ^{1,2,4} , Mihail Ipatov ^{1,2}, Valentina Zhukova ^{1,2,4} ,
Ricardo Lopez Anton ^{5,*}  and Arcady Zhukov ^{1,2,4,6} 

¹ Department of Polymers and Advanced Materials, Faculty of Chemistry, University of the Basque Country, UPV/EHU, 20018 San Sebastián, Spain

² Department of Applied Physics I, EIG, University of the Basque Country, UPV/EHU, 20018 San Sebastián, Spain

³ Physics Department, Faculty of Science, Sohag University, Sohag 82524, Egypt

⁴ EHU Quantum Center, University of the Basque Country, UPV/EHU, 20018 San Sebastián, Spain

⁵ Department of Applied Physics, Regional Institute for Applied Scientific Research (IRICA), University of Castilla-La Mancha, 13071 Ciudad Real, Spain

⁶ IKERBASQUE, Basque Foundation for Science, 48011 Bilbao, Spain

* Correspondence: mohamed.salaheldeenmohamed@ehu.eus (M.S.); ricardo.lopez@uclm.es (R.L.A.)

Abstract: In the current study we have obtained Co₂FeSi glass-coated microwires with different geometrical aspect ratios, $\rho = d/D_{\text{tot}}$ (diameter of metallic nucleus, d and total diameter, D_{tot}). The structure and magnetic properties are investigated at a wide range of temperatures. XRD analysis illustrates a notable change in the microstructure by increasing the aspect ratio of Co₂FeSi-glass-coated microwires. The amorphous structure is detected for the sample with the lowest aspect ratio ($\rho = 0.23$), whereas a growth of crystalline structure is observed in the other samples (aspect ratio $\rho = 0.30$ and 0.43). This change in the microstructure properties correlates with dramatic changing in magnetic properties. For the sample with the lowest ρ -ratio, non-perfect square loops are obtained with low normalized remanent magnetization. A notable enhancement in the squareness and coercivity are obtained by increasing ρ -ratio. Changing the internal stresses strongly affects the microstructure, resulting in a complex magnetic reversal process. The thermomagnetic curves show large irreversibility for the Co₂FeSi with low ρ -ratio. Meanwhile, if we increase the ρ -ratio, the sample shows perfect ferromagnetic behavior without irreversibility. The current result illustrates the ability to control the microstructure and magnetic properties of Co₂FeSi glass-coated microwires by changing only their geometric properties without performing any additional heat treatment. The modification of geometric parameters of Co₂FeSi glass-coated microwires allows to obtain microwires that exhibit an unusual magnetization behavior that offers opportunities to understand the phenomena of various types of magnetic domain structures, which is essentially helpful for designing sensing devices based on thermal magnetization switching.

Keywords: Heusler alloys; glass-coated microwires; multi-step magnetic behavior; sensing applications



Citation: Salaheldeen, M.; Wederni, A.; Ipatov, M.; Zhukova, V.; Lopez Anton, R.; Zhukov, A. Enhancing the Squareness and Bi-Phase Magnetic Switching of Co₂FeSi Microwires for Sensing Application. *Sensors* **2023**, *23*, 5109. <https://doi.org/10.3390/s23115109>

Academic Editor: Christer Johansson

Received: 11 April 2023

Revised: 13 May 2023

Accepted: 25 May 2023

Published: 26 May 2023



Copyright: © 2023 by the authors. Licensee MDPI, Basel, Switzerland. This article is an open access article distributed under the terms and conditions of the Creative Commons Attribution (CC BY) license (<https://creativecommons.org/licenses/by/4.0/>).

1. Introduction

The use of ferromagnetic materials in spintronic applications has garnered increasing attention in recent years due to their unique magnetic properties that enable the control and manipulation of spin currents. Among the different types of ferromagnetic materials, micro/nano-structured materials have emerged as promising candidates for enhancing spintronic devices' performance [1–9]. One of the most promising multidisciplinary research fields is spintronics, which enables the creation of the next generation of nano & microdevices with improved processing and memory capability while consuming less power [10]. To address the various required criteria, such as high spin polarization or high

Curie temperature, T_c , a new generation of materials with multifunction uses has to be created [11]. These Heusler compounds are well suited for spintronic and magneto-electronic applications [12]. Between the advantages of these compounds, we can highlight several ones: good lattice matching with the most typical substrates, T_c above room temperature, and the possibility of obtaining close to 100% of spin polarized near the Fermi level [11–15].

In particular, Co₂-based full-Heusler compounds are among the most promising half-metallic alloys due to their high thermal stability, high Curie temperatures ($T_c \approx 1100$ K) in bulk form, high magnetic moment ($\sim 6 \mu_B/\text{f.u.}$), and low Gilbert damping constant ($\alpha = 0.004$) [14,16,17]. Additionally, they exhibit interesting transport properties and high magnetic moments. It is noteworthy that these Co₂-based Heusler alloys present a significant anomalous Hall linked to the enormous Berry curvature associated with their band structure [16,18]. All the precedent evidence why the scientific community is so interested nowadays in Co-based full-Heusler alloys. Hence, these alloys are extensively researched in several configurations: nanoparticles [19], thin films [15,17,20], and nano/microwires [21–24]. It is relevant to note that the fabrication of Heusler alloys nanoparticles and thin films faces several difficulties for application purposes, including the high cost of preparation methods, chemical composition inhomogeneity, and ease of oxidation [20]. The diffusion of substrate atoms into the film results in the existence of the atomic disorder and phase separations, which are commonly observed [25], in addition to the lattice mismatch between the alloy and the substrate. Furthermore, in order to start the requisite structural ordering, the arc-melted or thin-film-formed Heusler alloys need lengthy, high-temperature annealing procedures [26].

Magnetic wire research has received a lot of interest during the last several decades [27]. The focus is on amorphous magnetic wires, which can exhibit unusual magnetic features such as spontaneous magnetic bistability or the Giant magnetoimpedance phenomenon [27,28]. Several manufacturing processes involving fast solidification can be used to create magnetic wires containing amorphous and/or nanocrystalline phases [27,28]. Nevertheless, only the Taylor-Ulitovsky manufacturing approach allows the preparation of magnetic microwires with the widest diameter range (from 0.2 to 100 μm) [27,28]. Such microwires are composites consisting of metallic nuclei (with $0.2 \leq d \leq 100 \mu\text{m}$) usually comprised of iron, cobalt, nickel, or their alloys, covered by thin, flexible, and insulating glass (typically Pyrex or Duran) coating (typically with thickness from 0.5 to 10 μm) [27,28]. As a result, the prospective applications of glass-coated microwires in sensing, actuation, and biomedical engineering have been expanded. The insulating and flexible glass coating protects the microwires from oxidation, corrosion, and other environmental factors while simultaneously giving them outstanding mechanical stability. Moreover, the glass layer and the magnetically flexible amorphous metallic nucleus provide high sensitivity to external stimuli including magnetic fields, temperature fluctuations, and mechanical stress [27–35]. Such sensitivity is connected to the ferromagnetic origin of the metallic nucleus, which responds to the applied stimulus. Innovative sensors that monitor magnetic fields, temperature, and stress have been developed using glass-coated microwires for a range of applications [27–29]. Additionally, they have shown potential characteristics for actuators and in medical applications, including cancer treatment (through magnetic hyperthermia) [29] and medicine administration. Future technological advancements can use glass-coated microwires because of their distinctive combination of properties [27,29].

In this article, we report an attempt to prepare Co₂FeSi glass-coated microwires with variable geometrical aspect ratios $\rho = d/D_{\text{tot}}$ (being d —diameter of the metallic nucleus and D_{tot} —total diameter). The fabrication method was chosen because of the interesting relationship between the magnetic and structural properties in the case of Heusler alloys in the form of glass-coated microwires, coupled with the properties provided by this fabrication method: excellent mechanical properties, insulating behavior, thin and flexible glass-coating, and small dimensionality [27,29–35]. As a result, we have prepared Co₂FeSi glass-coated microwires using the Taylor-Ulitovsky procedure, which is detailed previously [27,36,37]. The Taylor-Ulitovsky method, which has been fairly utilized since

the 1960s [37], is probably the most used fabrication method to make Heusler alloys glass-coated microwires with a wide variety of geometric characteristics [21,22,24,27–35]. The primary benefit of this non-expensive technique is that it allows the production of thin and long (up to several kilometers long) microwires with a wide diameter range (from 0.2 μm up to 100 μm) at a high rate (up to some hundred meters per minute) [36–38]. This process is also used to prepare glass-coated microwires with excellent mechanical properties [21,39–41]. Additional benefits of glass coating on microwires are better isolation and protection from the surroundings. Moreover, the fact that the glass coating is biocompatible, coupled with the commented properties, make this approach well-suited for biological applications [29,42,43]. Therefore, Heusler microwires of Co_2FeSi are an interesting material for a broad range of applications and devices. As far as we know, there is no report up to date on the production and structural, mechanical, or magnetic properties of Co_2FeSi -based glass-covered Heusler microwires with varied ρ -ratios, as well as the investigation of its influence on magneto-structure behavior.

2. Materials and Methods

Arc melting is a method of manufacturing Co_2FeSi alloys that involves melting the precursor components together in an electric arc furnace. Typically, the following procedures are used to create Co_2FeSi alloys by arc melting: (i) preparing the precursor ingredients. The precursor elements for the Co_2FeSi alloy are weighed and deposited in a graphite crucible, containing cobalt (powder) (99.99%), iron (powder) (99.9%), and silicon (powder) (99.99%) supplied by Technoamorf S.R.L. Co. (Cisineu, Moldavia). (ii) The materials melting. The crucible containing the precursor materials is put in an electric arc furnace, and an electrical current is fed through the materials to start the melting process in a vacuum and argon atmosphere. The furnace temperature is precisely regulated to ensure that the ingredients melt and mix equally. (iii) The cooling and solidification processes. The crucible is withdrawn from the furnace and allowed to cool once the components have melted and combined. The Co_2FeSi alloy (ingot) is created as the ingredients consolidate. This process was then repeated five times to achieve perfect homogeneity and a homogeneous microstructure. Once the Co_2FeSi alloy has solidified and formed an ingot, the ingot is used to prepare Co_2FeSi glass-coated microwires using the Taylor-Ulitovsky process. As described in the introduction, the Taylor-Ulitovsky preparation technique offers significant benefits over alternative procedures for manufacturing glass-coated microwires. One advantage is that it enables the fabrication of microwires with rather thin glass coatings, generally up to a few micrometers thick. This thin insulating coating permits the electrical and magnetic characteristics of the microwire metallic nucleus to be preserved, making the resultant microwires valuable for a wide range of applications. Many prior publications [21,22,24,27–35] explain the manufacturing method in detail. To summarize it, a glass capillary was filled with Co_2FeSi alloy, molten using a high frequency inductor for heating an ingot over its melting temperature. The variation of the speed of wire drawing, alloy temperature, glass tube feed rate and of the rotation of the pick-up bobbin were the parameters used to control the diameter of the metallic nuclei, d_{metal} (μm), and total diameter D_{total} (μm) as explained in detail elsewhere [38]. Finally, the microwire is cooled with a coolant stream to complete the rapid melt quenching process. All geometric parameters of samples investigated in current study are listed in Table 1, also including a similar sample previously studied (in ref. [24]), whose results will be also discussed in the following section.

Table 1. The geometrical parameters d_{metal} (μm), D_{total} (μm), aspect ratio, and average (Av.) of atomic percentage of Co, Fe, and Si elemental composition in Co_2FeSi glass-coated microwires.

Sample	d_{metal} (μm)	D_{total} (μm)	Aspect Ratio (ρ)	Chemical Composition
GCMW _A	5.1 ± 0.1	22.2 ± 0.1	0.23 ± 0.01	$\text{Co}_{44}\text{Fe}_{23}\text{Si}_{33}$
GCMW ^{**}	4.4 ± 0.1	17.6 ± 0.1	0.25 ± 0.01	$\text{Co}_{44}\text{Fe}_{23}\text{Si}_{33}$
GCMW _B	6.4 ± 0.1	21.3 ± 0.1	0.30 ± 0.01	$\text{Co}_{44}\text{Fe}_{23}\text{Si}_{33}$
GCMW _C	7.7 ± 0.1	17.9 ± 0.1	0.43 ± 0.01	$\text{Co}_{44}\text{Fe}_{23}\text{Si}_{33}$

GCMW^{**}: Co_2FeSi glass-coated microwires with ($\rho = 0.25$) [24].

We used Scanning Electron Microscopy (SEM) and Energy Dispersive X-ray (EDX) (JEOL-6610LV, JEOL Ltd., Tokyo, Japan) to determine the aspect ρ -ratio of Co_2FeSi glass-coated microwires samples and its related nominal chemical composition.

The XRD structure analysis was carried on by using X-ray diffraction (XRD) BRUKER (D8 Advance, Bruker AXS GmbH, Karlsruhe, Germany).

The magnetic behavior was studied in two different ways: hysteresis loops at temperatures between 5 and 350 K, and thermomagnetic curves following three different protocols, zero field cooling (ZFC), field cooling (FC), and field heating (FH) at the low magnetic field ($H = 200$ Oe). All magnetization curves were measured using a PPMS (Physical Property Magnetic System, Quantum Design Inc., San Diego, CA, USA) vibrating-sample magnetometer at temperatures, T , between 5 and 400 K for ZFC, FC, and FH magnetic curves. For the hysteresis loops, we only focus on the in-plane configuration where the applied magnetic field is parallel to the wire axis. The results are provided in terms of the normalized magnetization, $M/M_{5\text{K}}$, where $M_{5\text{K}}$ is the magnetic moment obtained at 5 K to avoid misleading of the estimation of the errors in the estimation of the magnetization saturation values.

3. Results

3.1. Analysis of Chemical and Structural Data

The geometries (ρ -ratios) and chemical compositions of prepared samples are shown in Table 1. The variation of the microwires diameters (d_{metal} and D_{total}) is achieved by controlling the drawing rate, alloy temperature, glass tube feed rate, and the receiving bobbin rotation speed [38]. Using the EDX data from Table 1, it was revealed that the metallic nucleus composition differed considerably from the stoichiometric one (Co_2FeSi). The features of the preparation process, which involved alloy melting and drawing, were the cause of this slight variation. To quantify the difference, we checked the nominal composition for eight sites as illustrated in Figure 1a. An atomic average of $\text{Co}_{44}\text{Fe}_{23}\text{Si}_{33}$ was used to confirm that the true 2:1 ratio of Co and Fe was applied in all sites. A high Si ratio was found because of the interfacial layer that exists between the metallic nucleus and the glass covering.

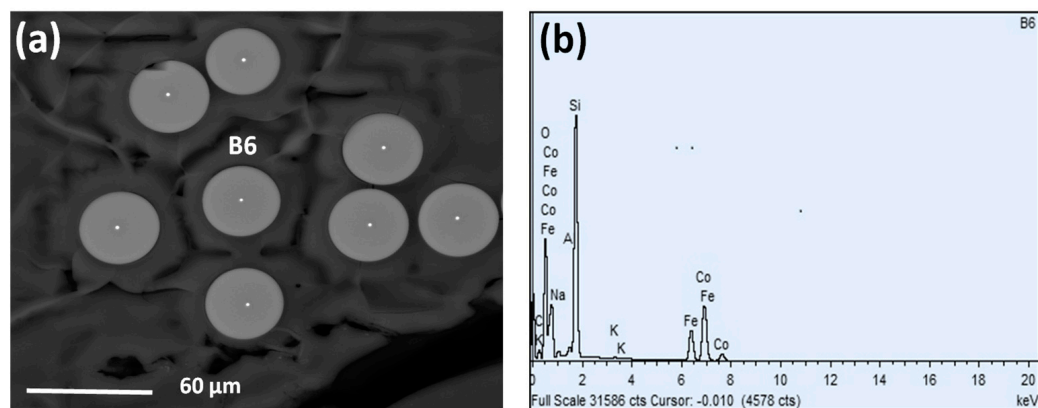


Figure 1. The cross section of selected Co_2FeSi glass-coated microwires with aspect ratio 0.30 images (a) and the chemical composition spectra of EDX of one of the points (b).

In order to study the order state of our produced Co_2FeSi glass-coated microwires, and to elucidate the effect of the aspect ratio modification on the crystalline structure, XRD structure analysis was carried on by using X-ray diffraction (XRD).

As illustrated in Figure 2, the change in the geometric ρ -ratio has a strong influence on the structure of Co_2FeSi glass-coated microwires. For the sample with the lowest ρ -ratio, i.e., $\rho = 0.25$, the sample shows an amorphous structure where no crystalline peaks are detected. The wide halo at $2\theta = 22.3^\circ$ is related to the glass coating layer, as reported in our previous works [21,22,24,27–35]. By increasing the geometric aspect ratio, a crystalline structure of the metallic nucleus becomes evident with a notable peak at $2\theta = 46.2^\circ$, attributing to the (220) reflection. Further increase of geometric ρ results in the perfect crystalline structure of samples studied, where the crystalline peak intensity increases and an additional peak appears at $2\theta = 85.4^\circ$, corresponding to the (422) reflection. The analysis of XRD profiles of the two crystalline Co_2FeSi samples, i.e., GCMW_C ($\rho = 0.30$) and GCMW_B ($\rho = 0.43$), indicates an A2 single-phase structure with a small tetragonal distortion (traces of tetragonal martensite phase), and a broadened peak around 22° attributed to an amorphous state for GCMW_C and mixed L2_1 or B2 phases with the amorphous state for GCMW_B sample [34,35].

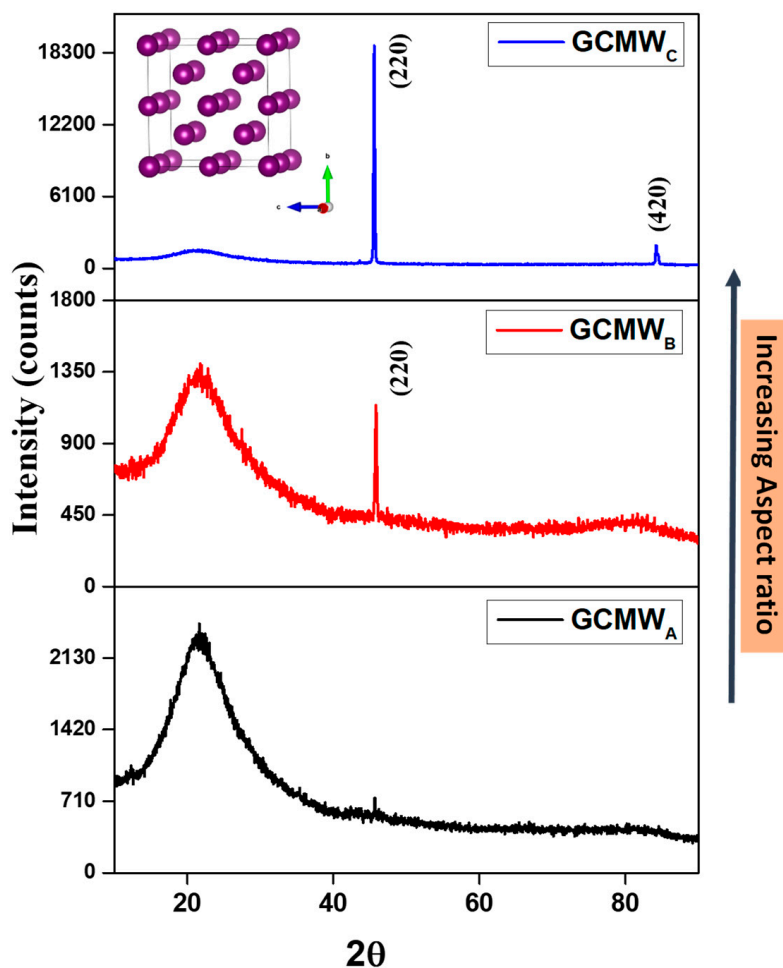


Figure 2. XRD analysis of Co_2FeSi glass-coated microwires with different aspect ratio measured at room temperature. The inset of Figure 2 indicates the A2-type cubic structure.

The (220) and (422) reflections in GCMW_C sample are split due to some tetragonal distortions of the crystal lattice. A similar phenomenon was seen and discussed elsewhere [44]. It is known that a split in the bragg diffraction patterns leads to a small distortion of the crystalline structure [45]. The absence of a (400) peak around 85° , which is expected to be present in the A2 structure, increases the possibility that the crystallites are too fine

to be detected by X-rays, as reported elsewhere [46]. In addition, the absence of some peaks can be caused by a similar scattering factor of the constituent elements (Co, Fe, and Si) [47]. Otherwise, according to the theoretical outcomes of Zhang et al., the disordered A2 state is more energetically preferable than those of the ordered L2₁ or B2 phases [48,49]. Nevertheless, the well-defined and sharp diffraction patterns in this sample (GCMW_C sample) indicate a high crystallinity, as compared with the other two XRD spectra. As the development of traces of the secondary phase (tetragonal martensite) can affect magnetic behavior, this will be explored in more detail in the following sections.

We estimated the lattice parameters of the two crystalline Co₂FeSi glass-coated microwires, and then we employed the Debye-Scherrer's equation, as presented in our previous work [23], to investigate the microstructure of Co₂FeSi in greater depth. Using this methodology, we can estimate the average grain size, D_g , associated with the principal peaks, which is approximately 17.8 nm, 37.6 nm, and 45.8 nm for GCMW^{**}, GCMW_B, and GCMW_C of Co₂FeSi microwires, respectively, as illustrated in Table 2. Thus, D_g has a monotonic increase with increasing the aspect ratio.

Table 2. The average grain size and lattice parameters of Co₂FeSi glass-coated microwires with different aspect ratios.

Sample	Average Grain Size (nm)	Lattice Parameters (Å)
GCMW _A	-	-
GCMW ^{**}	17.8 ± 0.1	5.64 ± 0.01
GCMW _B	37.6 ± 0.1	5.63 ± 0.01
GCMW _C	45.8 ± 0.1	2.81 ± 0.01

GCMW^{**}: Co₂FeSi glass-coated microwires with ($\rho = 0.25$) [24].

3.2. Magnetic Characterization

3.2.1. Room Temperature Magnetic Properties

Figure 3 shows the magnetic hysteresis loops of Co₂FeSi-glass-coated microwires with different ρ -ratios, obtained at room temperature with an applied magnetic field parallel to the microwire axis. All samples exhibit typical ferromagnetic behaviour, due to the high Curie point of Co₂FeSi alloy greater than 1100 K [46]. The sample with a low ρ -ratio exhibits soft magnetic properties with coercivity, H_c , around 14 Oe, and a non-square hysteresis loop shape (Figure 3a). However, the sample with the largest ρ -ratio shows almost perfectly square hysteresis loops with higher H_c (about 87 Oe), than Co₂FeSi with a low ρ -ratio (see Figure 3b,c). In addition, the hysteresis loop shows multistep magnetic behavior (indicated with arrows in Figure 3c). The almost square hysteresis loops for the GCMW_C microwire with normalized remanent, M_r , near 0.96 indicates the axial character of magnetic anisotropy with the easy axis of magnetization along the direction of the applied magnetic field. Thus, the increase in ρ -ratio affects the magnetocrystalline anisotropy, and its direction has the same direction of (220) and (420), as illustrated in the structural section. However, in the sample GCMW_B with a crystalline structure, non-perfectly square loops are observed. Such change in the hysteresis loop shape must be related to the presence of a considerable amount of amorphous phase beside the disordered B2 or little-ordered L2₁ structures. In our previous work at the same alloys, but with a low ρ -ratio ($\rho = 0.26$), the enhancement of the magnetocrystalline anisotropy, the squareness, and coercivity of Co₂FeSi glass-coated microwires after annealing was observed [21,22,24]. As we illustrated in our previous work, the two main factors affecting the magnetic anisotropy behavior in Heusler-based glass-coated microwires are uniaxial magnetic anisotropy and cubic magnetocrystalline anisotropy [21,22,24]. By increasing the ρ -ratio, an enhancement in the crystalline phase content correlates with the magnetic property modification, i.e., the main factor controlling the magnetic anisotropy is the cubic magnetocrystalline anisotropy. Unfortunately, currently, we are not able to measure this type of anisotropy experimentally, but the perfectly square loop indicates its strong effect on the GCMW_B and GCMW_C samples. As seen in Figure 4, the GCMW_C sample shows the highest anisotropy field

H_k , coercivity H_c , and normalized remnant M_r . The odd behavior of H_k is likely related to the big amorphous phase present in $GCMW_A$ and $GCMW_B$ samples, as the behavior of H_c for these two samples is also quite similar (there is not a decrease, as in the case of the H_k , but the values are almost the same) and maybe the growth of the crystalline structure eases initially the reduction of the anisotropy field. In addition, the different types of microstructures (L21, B2, and A2) can also strongly affect the H_k behavior.

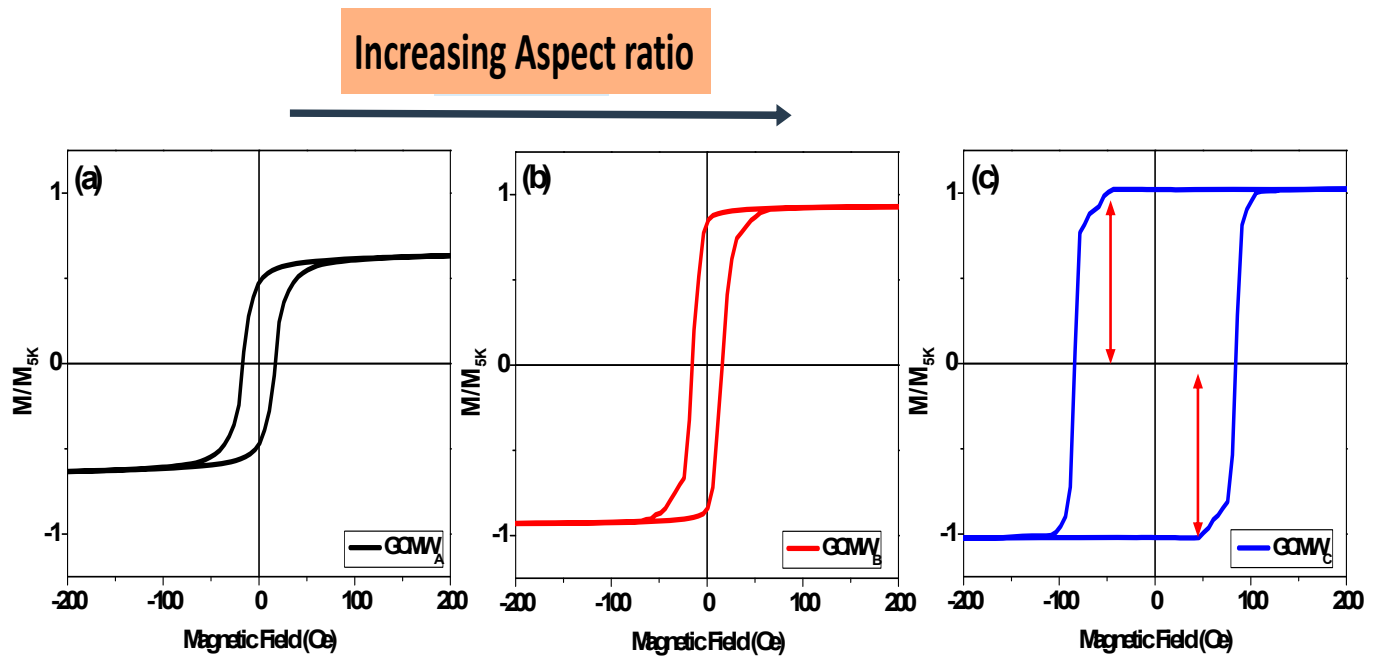


Figure 3. Room temperature hysteresis loops for Co_2FeSi glass-coated microwires (a) $GCMW_A$, (b) $GCMW_B$, and (c) $GCMW_C$. The arrows in (c) pinpoint the multistep magnetic behavior.

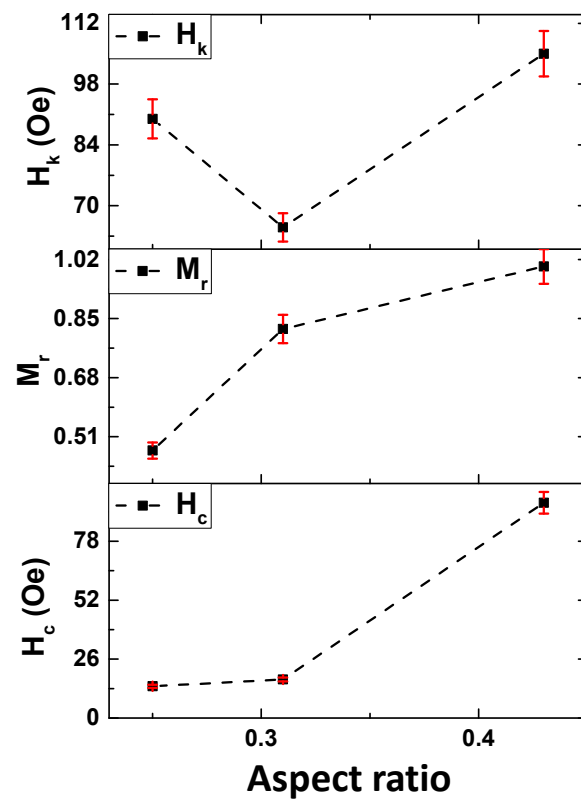


Figure 4. Aspect ratio dependence on coercivity (H_c), normalized remanence (M_r), and in-plane anisotropy field (H_k) of Co_2FeSi glass-coated microwires (lines for eye guide).

3.2.2. Thermomagnetic Properties

It is worth noting that the ferromagnetic materials temperature stability is a crucial characteristic for their possible applications in spintronic and sensing devices. Hence, for a wide range of measurement temperatures, 5–350 K, we investigated the magnetic behavior of Co_2FeSi glass-coated microwires with different ρ -ratios. The shape of the loops follows the same trend observed at room temperature: non-square for the GCMW_A sample, quite square for the GCMW_B one, and almost square for the GCMW_C one (loops not shown). In Figure 5, the evolution of H_c and M_r with the temperature is shown. This behavior demonstrates that for the GCMW_C sample, cubic magnetocrystalline anisotropy prevails up to 350 K.

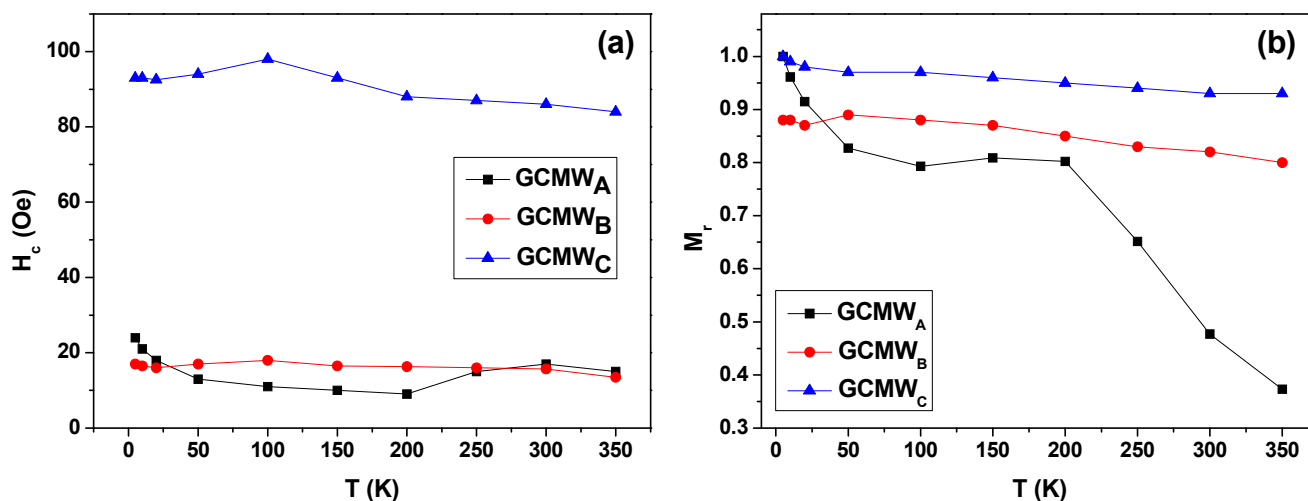


Figure 5. Temperature dependence of the coercivity (a) and normalized remanence (b) of Co_2FeSi glass-coated microwires with different aspect ratio (lines for eye guide). The error bar is as big or smaller than the size of the symbols.

By analyzing the hysteresis loops measured at temperature range, 5–350 K of Co_2FeSi glass-coated microwires with different ρ -ratio, an interesting magnetic behavior is found for both the temperature dependence of H_c and of the normalized remanence, M_r . GCMW_C sample shows the highest value of the coercivity at the all measuring range of temperature range, with an average value of H_c six times higher than those of the GCMW^{**} , GCMW_A and GCMW_B samples. GCMW^{**} , GCMW_A , and GCMW_B samples show quite similar values of the H_c where the difference between the average value of coercivity is about 2 Oe. By estimating the differences in the coercivity (ΔH_c) between the maximum value of coercivity ($H_{c(\max)}$) and the lowest value of the coercivity ($H_{c(\min)}$) for all samples, we pretend to show its stability with temperature. The samples with a clear crystalline phase, GCMW^{**} , GCMW_B , and GCMW_C samples, show higher temperature stability than the amorphous GCMW_A sample. Hence, the ΔH_c is 11 Oe, 3.5, and 9 Oe for GCMW^{**} , GCMW_B , and GCMW_C samples, respectively, whereas ΔH_c is 15 Oe for the GCMW_A one. The magnetic stability is clearer in the case of M_r tendency with the temperature of Co_2FeSi glass-coated microwires with different ρ -ratios. As shown in Figure 5b, both GCMW_B and GCMW_C samples show high stability with temperature, with ΔM_r 0.05 and 0.06, respectively (see Table 3). Meanwhile, the behavior of M_r of GCMW_A is rather different, compared to the other samples with higher ρ -ratios, where a monotonic increase with decreasing the temperature has been observed.

Table 3. The geometrical parameters and average (Av.) of Co_2FeSi glass-coated microwires with different aspect ratios.

Sample	$\Delta H_c (H_{c(\max)} - H_{c(\min)})$	$\Delta M_r (M_{r(\max)} - M_{r(\min)})$
GCMW_A	15 ± 2 Oe	0.7 ± 0.1
GCMW^{**}	11 ± 1 Oe	0.6 ± 0.1
GCMW_B	3.5 ± 0.5 Oe	0.06 ± 0.01
GCMW_C	9 ± 2 Oe	0.05 ± 0.01

GCMW^{**} : Co_2FeSi glass-coated microwires with ($\rho = 0.25$) [24].

Figure 6 shows the complete thermomagnetic behavior of Co_2FeSi glass-coated microwires with different ρ -ratios. We performed the ZFC, FC, and FH magnetic temperature dependence to check any possible phase transition. Thus, the measurements were performed at a low magnetic field of 200 Oe. For the GCMW_A sample, the ZFC, FC, and FH magnetizations curves show non-homogenous behavior, besides an irreversible magnetic behavior at $T = 150$ K. Such irreversibility has been observed in our previous work deal-

ing with Co₂FeSi-based glass-coated microwires with aspect ratio $\rho = 0.25$, i.e., GCMW**, (see [21,22,24]). In this work, we have illustrated that the irreversibility is enhanced by performing annealing at 873 K and 973 K for 1 h. The induced martensitic transition and the change in the internal stresses associated with the glass-covering layer with temperature allow to control the irreversibility behavior. The interesting point for Co₂FeSi glass-coated microwires with the lowest ρ -ratio, i.e., $\rho = 0.23$, is that its blocking temperature is observed at $T = 150$ K, such as the Co₂FeSi glass-coated microwires with $\rho = 0.25$, i.e., GCMW** [21,22,24]. For the GCMW_A sample, which is totally in an amorphous state (see Figure 2), the main reason for the irreversibility behavior is the strong internal stress induced by the glass covering layer. For GCMW_B and GCMW_C samples, with increasing ρ -ratio, the irreversibility behavior disappeared, and the usual ferromagnetic behavior is observed with homogenous ZFC, FC, and FH magnetic curves. The homogenous magnetization curves are due to the induced crystal structure with A2-type and B2 or L2₁ cubic structure for GCMW_C and GCMW_B, respectively.

We believe that increasing the ρ -ratio of Co₂FeSi glass-coating microwires affects recrystallization, atomic ordering, and stress reduction. Furthermore, for samples with a high ρ -ratio, the induced L2₁/B2 and A2 cubic structure types generate a strong magneto crystalline anisotropy, explaining the behavior of magnetic properties such as H_c , M_r , H_k , and thermomagnetic curves with temperature. In fact, as shown in several previous publication, the internal stress values are affected by the ρ -ratio: the lower the ρ -ratio, the higher the internal stresses related to the presence of the glass-coating [50–52]. On the other hand, the glass-coating thermal conductivity can affect the quenching rate of the metallic nucleus: a lower quenching rate must be at the origin of higher crystallinity of the microwires with relatively thick glass-coating [27]. The aforementioned internal stresses together with the samples' microstructure (average grain size) can affect the hysteresis loops. Additionally, the presence of the interfacial layer between the metallic nucleus and glass-coating, reported by us earlier can affect the saturation magnetization [53]. Such influence of the interfacial layer must be more appreciable for the thinner d_{metal} -values.

In summary, Co₂FeSi glass-coated microwires are an excellent candidate for a wide range of industrial applications, especially for sensors, due to their perfect squared loops at a wide temperature range and homogenous thermomagnetic behavior with temperature.

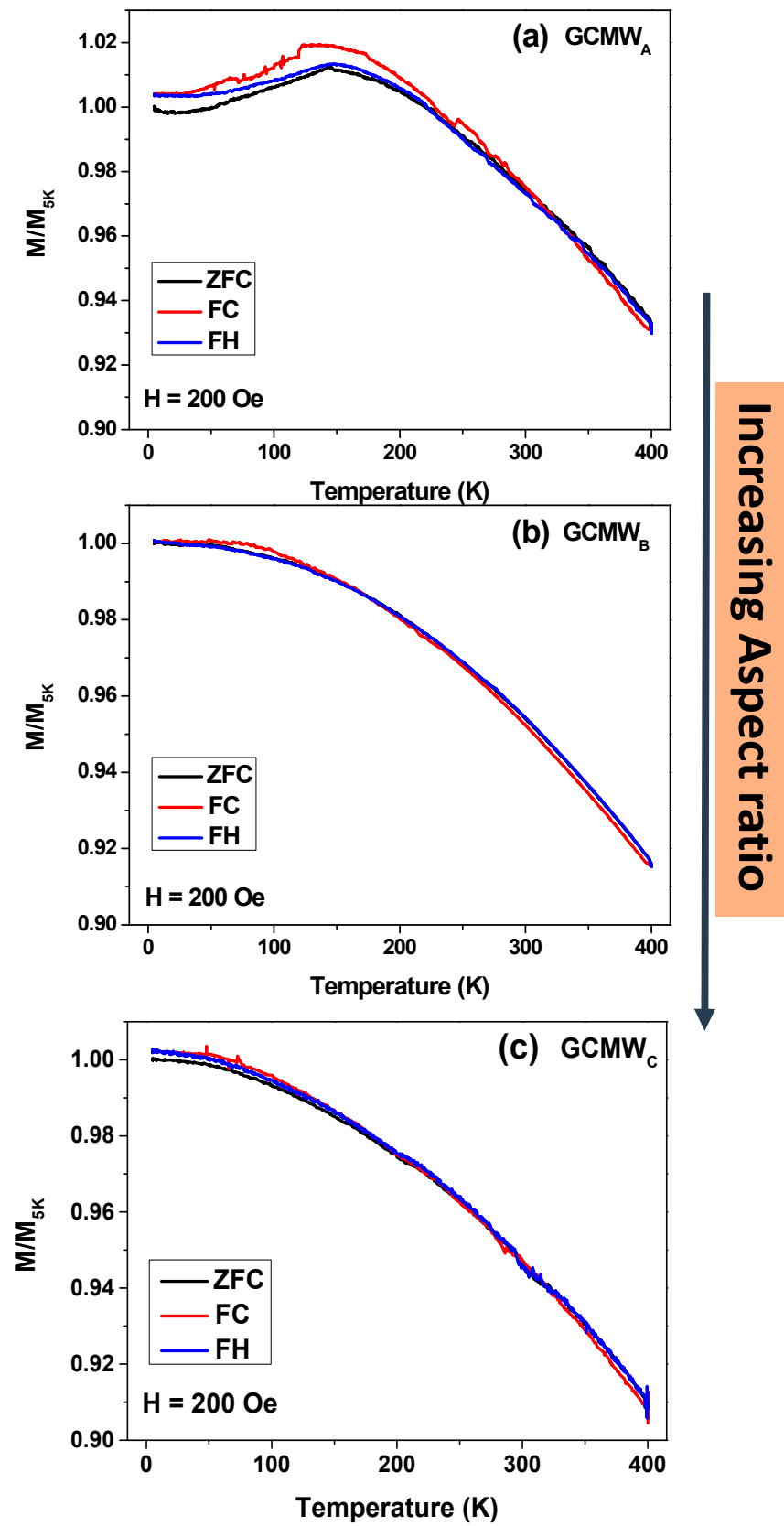


Figure 6. Temperature dependence of magnetization measured for Co₂FeSi glass-coated microwires (a) GCMW_A, (b) GCMW_B, and (c) GCMW_C with applied external magnetic field 200 Oe.

4. Conclusions

In summary, we have fabricated Co₂FeSi-glass-coated microwires with different geometrical aspect ratios. A strong influence of the geometric aspect ratio on the magnetic and structural properties is observed and discussed. The increase in the aspect ratio correlates with the increasing degree of crystallinity. Promising coercivity and normalized remnant stability with temperature are found for Co₂FeSi glass-coated microwires with a high aspect ratio. For the sample with the lowest aspect ratio, the thermomagnetic curves show large irreversibility with a blocking temperature of $T = 150$ K. The induced crystal structure of the A2-type gives rise to a high cubic magnetocrystalline anisotropy that controls the magnetic behavior of Co₂FeSi glass-coated microwires and makes it a suitable candidate for magnetic sensing.

Author Contributions: Conceptualization, M.S. and A.Z.; methodology, V.Z.; validation, M.S., V.Z. and A.Z.; formal analysis, M.S. and A.W.; investigation, M.S., A.W. and A.Z.; resources, V.Z. and A.Z.; data curation, M.I.; writing—original draft preparation, M.S., A.W. and A.Z.; writing—review and editing, M.S., R.L.A. and A.Z.; visualization, M.S., A.W. and M.I.; supervision, R.L.A. and A.Z.; project administration, V.Z. and A.Z.; funding acquisition, V.Z. and A.Z. All authors have read and agreed to the published version of the manuscript.

Funding: This research was funded by the Spanish MICIN, under PID2022-141373NBI00, by EU under “INFINITE” (Horizon Europe) project and by the Government of the Basque Country, under PUE_2021_1_0009 and Elkartek (MINERVA, ZE-KONP and MAGAF) projects and by under the scheme of “Ayuda a Grupos Consolidados” (Ref.: IT1670-22). MS wish to acknowledge the funding within the Maria Zambrano contract by the Spanish Ministerio de Universidades and European Union –Next Generation EU (“Financiado por la Unión Europea-Next Generation EU”). We also wish to thank the administration of the University of the Basque Country, which not only provides very limited funding, but even expropriates the resources received by the research group from private companies for the research activities of the group. Such interference helps keep us on our toes.

Institutional Review Board Statement: Not applicable.

Informed Consent Statement: Not applicable.

Data Availability Statement: Not applicable.

Acknowledgments: The authors thank for technical and human support provided by SGIker Magnetic Measurements Gipuzkoa (UPV/EHU/ ERDF, EU).

Conflicts of Interest: The authors declare no conflict of interest.

References

1. Li, T.; Pickel, A.D.; Yao, Y.; Chen, Y.; Zeng, Y.; Lacey, S.D.; Li, Y.; Wang, Y.; Dai, J.; Wang, Y.; et al. Thermoelectric properties and performance of flexible reduced graphene oxide films up to 3000 K. *Nat. Energy* **2018**, *3*, 148–156. [\[CrossRef\]](#)
2. Hoop, M.; Ribeiro, A.S.; Rösch, D.; Weinand, P.; Mendes, N.; Mushtaq, F.; Chen, X.Z.; Shen, Y.; Pujante, C.F.; Puigmartí-Luis, J.; et al. Mobile Magnetic Nanocatalysts for Bioorthogonal Targeted Cancer Therapy. *Adv. Funct. Mater.* **2018**, *28*, 1705920. [\[CrossRef\]](#)
3. Saccone, M.; Scholl, A.; Velten, S.; Dhuey, S.; Hofhuis, K.; Wuth, C.; Huang, Y.-L.; Chen, Z.; Chopdekar, R.V.; Farhan, A. Towards artificial Ising spin glasses: Thermal ordering in randomized arrays of Ising-type nanomagnets. *Phys. Rev. B* **2020**, *99*, 224403. [\[CrossRef\]](#)
4. Salahldeen, M.; Nafady, A.; Abu-Dief, A.M.; Díaz Crespo, R.; Fernández-García, M.P.; Andrés, J.P.; López Antón, R.; Blanco, J.A.; Álvarez-Alonso, P. Enhancement of Exchange Bias and Perpendicular Magnetic Anisotropy in CoO/Co Multilayer Thin Films by Tuning the Alumina Template Nanohole Size. *Nanomaterials* **2022**, *12*, 2544. [\[CrossRef\]](#) [\[PubMed\]](#)
5. Kiwi, M. Exchange Bias Theory. *J. Magn. Magn. Mater.* **2001**, *234*, 584–595. [\[CrossRef\]](#)
6. Skjærvø, S.H.; Marrows, C.H.; Stamps, R.L.; Heyderman, L.J. Advances in artificial spin ice. *Nat. Rev. Phys.* **2019**, *2*, 13–28. [\[CrossRef\]](#)
7. Maniv, E.; Murphy, R.A.; Haley, S.C.; Doyle, S.; John, C.; Maniv, A.; Ramakrishna, S.K.; Tang, Y.-L.; Ercius, P.; Ramesh, R.; et al. Exchange bias due to coupling between coexisting antiferromagnetic and spin-glass orders. *Nat. Phys.* **2021**, *17*, 525–530. [\[CrossRef\]](#)
8. Meiklejohn, W.H.; Bean, C.P. New Magnetic Anisotropy. *Phys. Rev.* **1957**, *105*, 904–913. [\[CrossRef\]](#)
9. Yang, S.-H.; Ryu, K.-S.; Parkin, S. Domain-wall velocities of up to 750 m s⁻¹ driven by exchange-coupling torque in synthetic antiferromagnets. *Nat. Nanotechnol.* **2015**, *10*, 221–226. [\[CrossRef\]](#)

10. Elphick, K.; Frost, W.; Samiepour, M.; Kubota, T.; Takanashi, K.; Sukegawa, H.; Mitani, S.; Hirohata, A. Heusler Alloys for Spintronic Devices: Review on Recent Development and Future Perspectives. *Sci. Technol. Adv. Mater.* **2021**, *22*, 235–271. [[CrossRef](#)]
11. Tavares, S.; Yang, K.; Meyers, M.A. Heusler alloys: Past, properties, new alloys, and prospects. *Prog. Mater. Sci.* **2023**, *132*, 101017. [[CrossRef](#)]
12. De Groot, R.A.; Mueller, F.M.; Engen, P.G.V.; Buschow, K.H.J. New Class of Materials: Half-Metallic Ferromagnets. *Phys. Rev. Lett.* **1983**, *50*, 2024. [[CrossRef](#)]
13. Bai, Z.; Shen, L.E.I.; Han, G.; Feng, Y.P. Data Storage: Review of Heusler Compounds. *Spin* **2012**, *2*, 1230006. [[CrossRef](#)]
14. Balke, B.; Wurmehl, S.; Fecher, G.H.; Felser, C.; Kübler, J. Rational Design of New Materials for Spintronics: Co_2FeZ (Z=Al, Ga, Si, Ge). *Sci. Technol. Adv. Mater.* **2008**, *9*, 014102. [[CrossRef](#)] [[PubMed](#)]
15. Hirohata, A.; Sagar, J.; Lari, L.; Fleet, L.R.; Lazarov, V.K. Heusler-alloy films for spintronic devices. *Appl. Phys. A* **2013**, *111*, 423–430. [[CrossRef](#)]
16. Li, P.; Koo, J.; Ning, W.; Li, J.; Miao, L.; Min, L.; Zhu, Y.; Wang, Y.; Alem, N.; Liu, C.X.; et al. Giant Room Temperature Anomalous Hall Effect and Tunable Topology in a Ferromagnetic Topological Semimetal Co_2MnAl . *Nat. Commun.* **2020**, *11*, 3476. [[CrossRef](#)]
17. Jourdan, M.; Minár, J.; Braun, J.; Kronenberg, A.; Chadov, S.; Balke, B.; Gloskovskii, A.; Kolbe, M.; Elmers, H.J.; Schönhense, G.; et al. Direct Observation of Half-Metallicity in the Heusler Compound Co_2MnSi . *Nat. Commun.* **2014**, *5*, 3974. [[CrossRef](#)]
18. Guillemard, C.; Petit-Watlot, S.; Pasquier, L.; Pierre, D.; Ghanbaja, J.; RojasSánchez, J.C.; Bataille, A.; Rault, J.; le Fèvre, P.; Bertran, F.; et al. Ultralow Magnetic Damping in Co_2Mn -Based Heusler Compounds: Promising Materials for Spintronics. *Phys. Rev. Appl.* **2019**, *11*, 064009. [[CrossRef](#)]
19. Nehla, P.; Ulrich, C.; Dhaka, R.S. Investigation of the Structural, Electronic, Transport and Magnetic Properties of Co_2FeGa Heusler Alloy Nanoparticles. *J. Alloys Compd.* **2019**, *776*, 379–386. [[CrossRef](#)]
20. Patra, N.; Prajapat, C.L.; Babu, P.D.; Rai, S.; Kumar, S.; Jha, S.N.; Bhattacharyya, D. Pulsed Laser Deposited Co_2FeSi Heusler Alloy Thin Films: Effect of Different Thermal Growth Processes. *J. Alloys Compd.* **2019**, *804*, 470–485. [[CrossRef](#)]
21. Salaheldeen, M.; Ipatov, M.; Zhukova, V.; García-Gomez, A.; Gonzalez, J.; Zhukov, A. Preparation and magnetic properties of Co_2 -based Heusler alloy glass-coated microwires with high Curie temperature. *AIP Adv.* **2023**, *13*, 025325. [[CrossRef](#)]
22. Salaheldeen, M.; Garcia, A.; Corte-Leon, P.; Ipatov, M.; Zhukova, V.; Zhukov, A. Unveiling the Effect of Annealing on Magnetic Properties of Nanocrystalline Half-Metallic Heusler Co_2FeSi Alloy Glass-Coated Microwires. *J. Mater. Res. Technol.* **2022**, *20*, 4161–4172. [[CrossRef](#)]
23. Salaheldeen, M.; Ipatov, M.; Corte-Leon, P.; Zhukova, V.; Zhukov, A. Effect of Annealing on the Magnetic Properties of Co_2MnSi -Based Heusler Alloy Glass-Coated Microwires. *Metals* **2023**, *13*, 412. [[CrossRef](#)]
24. Salaheldeen, M.; Garcia-Gomez, A.; Ipatov, M.; Corte-Leon, P.; Zhukova, V.; Blanco, J.M.; Zhukov, A. Fabrication and MagnetoStructural Properties of Co_2 -Based Heusler Alloy Glass-Coated Microwires with High Curie Temperature. *Chemosensors* **2022**, *10*, 225. [[CrossRef](#)]
25. Khovaylo, V.V.; Rodionova, V.V.; Shevyrtalov, S.N.; Novosad, V. Magnetocaloric Effect in “Reduced” Dimensions: Thin Films, Ribbons, and Microwires of Heusler Alloys and Related Compounds. *Phys. Status Solidi* **2014**, *251*, 2104–2113. [[CrossRef](#)]
26. Belmeguenai, M.; Tuzcuoglu, H.; Gabor, M.S.; Petrisor, T.; Tiusan, C.; Zighem, F.; Chérif, S.M.; Moch, P. Co_2FeAl Heusler Thin Films Grown on Si and MgO Substrates: Annealing Temperature Effect. *J. Appl. Phys.* **2014**, *115*, 043918. [[CrossRef](#)]
27. Zhukov, A.; Corte-Leon, P.; Gonzalez-Legarreta, L.; Ipatov, M.; Blanco, J.M.; Gonzalez, A.; Zhukova, V. Advanced Functional Magnetic Microwires for Technological Applications. *J. Phys. D Appl. Phys.* **2022**, *55*, 253003. [[CrossRef](#)]
28. Chiriac, H.; Ovari, T.A. Amorphous glass-covered magnetic wires: Preparation, properties, applications. *Prog. Mater. Sci.* **1996**, *40*, 333–407. [[CrossRef](#)]
29. Mitxelena-Iribarren, O.; Campisi, J.; de Apellániz, I.M.; Lizarbe-Sancha, S.; Arana, S.; Zhukova, V.; Mujika, M.; Zhukov, A. Glass-coated ferromagnetic microwire-induced magnetic hyperthermia for in vitro cancer cell treatment. *Mater. Sci. Eng. C* **2020**, *106*, 110261. [[CrossRef](#)]
30. Salaheldeen, M.; Garcia-Gomez, A.; Corte-León, P.; Gonzalez, A.; Ipatov, M.; Zhukova, V.; Gonzalez, J.M.; López Antón, R.; Zhukov, A. Manipulation of Magnetic and Structure Properties of Ni_2FeSi Glass-Coated Microwires by Annealing. *J. Alloys Compd.* **2023**, *942*, 169026. [[CrossRef](#)]
31. Salaheldeen, M.; Talaat, A.; Ipatov, M.; Zhukova, V.; Zhukov, A. Preparation and Magneto-Structural Investigation of Nanocrystalline CoMn -Based Heusler Alloy Glass-Coated Microwires. *Processes* **2022**, *10*, 2248. [[CrossRef](#)]
32. Salaheldeen, M.; Garcia-Gomez, A.; Corte-Leon, P.; Ipatov, M.; Zhukova, V.; Gonzalez, J.; Zhukov, A. Anomalous Magnetic Behavior in Half-Metallic Heusler Co_2FeSi Alloy Glass-Coated Microwires with High Curie Temperature. *J. Alloys Compd.* **2022**, *923*, 166379. [[CrossRef](#)]
33. Hannel, M.; Varga, M.; Frolova, L.; Nalevanko, S.; Ibarra-Gaytán, P.; Vidyasagar, R.; Sarkar, P.; Dzubinska, A.; Galdun, L.; Ryba, T.; et al. Heusler-Based Cylindrical Micro- and Nanowires. *Phys. Status Solidi A* **2022**, *219*, 2100657. [[CrossRef](#)]
34. Salaheldeen, M.; Wederni, A.; Ipatov, M.; Gonzalez, J.; Zhukova, V.; Zhukov, A. Elucidation of the Strong Effect of the Annealing and the Magnetic Field on the Magnetic Properties of Ni_2 -Based Heusler Microwires. *Crystals* **2022**, *12*, 1755. [[CrossRef](#)]
35. Salaheldeen, M.; Wederni, A.; Ipatov, M.; Zhukova, V.; Zhukov, A. Preparation and Magneto-Structural Investigation of High-Ordered (L_2_1 Structure) Co_2MnGe Microwires. *Processes* **2023**, *11*, 1138. [[CrossRef](#)]

36. Zhukov, A.; Chichay, K.; Talaat, A.; Rodionova, V.; Blanco, J.M.; Ipatov, M.; Zhukova, V. Manipulation of magnetic properties of glass-coated microwires by annealing. *J. Magn. Magn. Mater.* **2015**, *383*, 232–236. [[CrossRef](#)]
37. Ulitovsky, A.V.; Maianski, I.M.; Avramenco, A.I. 1960 Method of Continuous Casting of Glass Coated Microwire. USSR Patent 128427, 6 May 2015. Bulletin, No 10, p. 14.
38. Larin, V.S.; Torcunov, A.V.; Zhukov, A.; Gonzalez, J.; Vazquez, M.; Panina, L. Preparation and Properties of Glass-coated Microwires. *J. Magn. Magn. Mater.* **2002**, *249*, 39–45. [[CrossRef](#)]
39. Chiriac, H.; Lupu, N.; Stoian, G.; Ababei, G.; Corodeanu, S.; Óvári, T.A. Ultrathin Nanocrystalline Magnetic Wires. *Crystals* **2017**, *7*, 48. [[CrossRef](#)]
40. Dufay, B.; Saez, S.; Dolabdjian, C.; Melo, L.G.C.; Yelon, A.; Ménard, D. Development of a high sensitivity Giant Magneto-Impedance magnetometer: Comparison with a commercial Flux-Gate. *IEEE Trans. Magn.* **2013**, *49*, 85. [[CrossRef](#)]
41. Goto, T.; Nagano, M.; Wehara, N. Mechanical properties of amorphous Fe₈₀P₁₆C₃B₁ filament produced by glass-coated melt spinning. *Trans. JIM* **1977**, *18*, 759–764. [[CrossRef](#)]
42. Zhukova, V.; Cobeño, A.F.; Zhukov, A.; de Arellano Lopez, A.R.; López-Pombero, S.; Blanco, J.M.; Larin, V.; Gonzalez, J. Correlation between magnetic and mechanical properties of devitrified glass-coated Fe_{71.8}Cu₁Nb_{3.1}Si₁₅B_{9.1} microwires. *J. Magn. Magn. Mater.* **2002**, *249*, 79–84. [[CrossRef](#)]
43. Kozejova, D.; Fecova, L.; Klein, P.; Sabol, R.; Hudak, R.; Sulla, I.; Mudronova, D.; Galik, J.; Varga, R. Biomedical applications of glass-coated microwires. *J. Magn. Magn. Mater.* **2019**, *470*, 2–5. [[CrossRef](#)]
44. Talaat, A.; Alonso, J.; Zhukova, V.; Garaio, E.; García, J.A.; Srikanth, H.; Phan, M.H.; Zhukov, A. Ferromagnetic Glass-Coated Microwires with Good Heating Properties for Magnetic Hyperthermia. *Sci. Rep.* **2016**, *6*, 39300. [[CrossRef](#)]
45. Kudryavtsev, Y.V.; Lee, Y.P.; Lee, N.N.; Huang, M.D. Effect of Structural Disorder on the Magnetic, Magneto-Optical and Optical Properties of the Ni₂MnIn Heusler Alloy Films. *Mater. Sci. Forum* **2005**, *480–481*, 623–628. [[CrossRef](#)]
46. Dubowik, J.; Kudryavtsev, Y.; Lee, Y.P.; Lee, N.N.; Hong, B.S. Influence of structural order on magnetic properties of ni₂mnin heusler alloy films. *Mol. Phys. Rep.* **2004**, *40*, 55–61.
47. Wang, K.; Xu, Z.; Fu, X.; Lu, Z.; Xiong, R. Magnetic and Structural Properties of Sputtered Thick Co₂FeSi Alloy Films. *J. Magn. Magn. Mater.* **2023**, *570*, 170557. [[CrossRef](#)]
48. Zhang, X.; Han, L.; Dehm, G.; Liebscher, C.H. Microstructure and Physical Properties of Dual-Phase Soft Magnetic Fe-Co-Ti-Ge Alloys. *J. Alloys Compd.* **2023**, *945*, 169282. [[CrossRef](#)]
49. Zhang, H.G.; Song, B.T.; Chen, J.; Yue, M.; Liu, E.K.; Wang, W.H.; Wu, G.H. Magnetization Variation in Fe–Cr–Ga System. *Intermetallics* **2019**, *113*, 106580. [[CrossRef](#)]
50. Xiao, A.; Zhou, Z.; Qian, Y.; Wang, X. Direct Observation of Evolution from Amorphous Phase to Strain Glass. *Materials* **2022**, *15*, 7900. [[CrossRef](#)]
51. Zhukov, A.; Gonzalez, J.; Torcunov, A.; Pina, E.; Prieto, M.J.; Cobeño, A.F.; Blanco, J.M.; Larin, V.; Baranov, S. Ferromagnetic resonance and Structure of Fe-based glass-coated Microwires. *J. Magn. Magn. Mater.* **1999**, *203*, 238–240. [[CrossRef](#)]
52. Chiriac, H.; Ovari, T.A.; Pop, G.; Barariu, F. Internal stresses in highly magnetostrictive glass-covered amorphous wires. *J. Magn. Magn. Mater.* **1996**, *160*, 237–238. [[CrossRef](#)]
53. Zhukov, A.; Shuvaeva, E.; Kaloshkin, S.; Churyukanova, M.; Kostitcyna, E.; Zhdanova, M.; Talaat, A.; Ipatov, M.; Zhukova, V. Studies of interfacial layer and its effect on magnetic properties of glass-coated microwires. *J. Electr. Mater.* **2016**, *45*, 2381–2387. [[CrossRef](#)]

Disclaimer/Publisher’s Note: The statements, opinions and data contained in all publications are solely those of the individual author(s) and contributor(s) and not of MDPI and/or the editor(s). MDPI and/or the editor(s) disclaim responsibility for any injury to people or property resulting from any ideas, methods, instructions or products referred to in the content.